

Wavelength-dependent photooxidation and photoreduction of protochlorophyllide and protochlorophyll in the innermost leaves of cabbage (*Brassica oleracea* var. *capitata* L.)

Anna Laura Erdei¹ · Annamária Kósa¹ · Lilla Kovács-Smirová¹ · Béla Böddi¹

Received: 17 March 2015 / Accepted: 19 October 2015 / Published online: 30 October 2015
© Springer Science+Business Media Dordrecht 2015

Abstract The photoreduction and photooxidation processes of different protochlorophyll(ide) forms were studied in the innermost leaves of cabbage (*Brassica oleracea* var. *capitata* L.) under monochromatic irradiations. Room-temperature fluorescence emission spectra were measured from the same leaf spots before and after illumination to follow the wavelength dependence of the photochemical reactions. Short-wavelength light of 7 $\mu\text{mol photons m}^{-2} \text{s}^{-1}$ (625–630 nm) provoked mainly bleaching, and longer wavelengths (630–640 nm) caused both bleaching and photoreduction, while above 640 nm resulted in basically photoreduction. When bleached leaves were kept in darkness at room temperature, all protochlorophyll(ide) forms regenerated during 72 h. Oxygen-reduced environment decreased the extent of bleaching suggesting the involvement of reactive oxygen species. These results confirm that the short-wavelength, 628 nm absorbing, and 633 nm emitting protochlorophyll(ide) form in etiolated cabbage leaves sensibilizes photooxidation. However, the 628 nm light at low intensities stimulates the photoreduction of the longer wavelength protochlorophyllide forms. Kinetic measurements showed that photoreduction saturates at a low PFD (photon flux density) compared to bleaching, suggesting that the quantum yield of photoreduction is higher than that of bleaching.

Keywords Action spectra · Bleaching · Cabbage innermost leaves · Photooxidation · Protochlorophyllide photoreduction

Abbreviations

Chl	Chlorophyll
Chlide	Chlorophyllide
L-POR	Light-dependent NADPH:protochlorophyllide oxidoreductase enzyme
Pchl	Protochlorophyll
Pchlde	Protochlorophyllide
PFD	Photon flux density
ROS	Reactive oxygen species

Introduction

The chlorophyll (Chl) biosynthesis of higher plants is light dependent; the pathway is arrested at the precursor protochlorophyllide (Pchlde) in dark developing tissues. The main steps of the porphyrin ring biosynthesis have been clarified (see for review Tanaka and Tanaka 2007), and plenty of details have been described about the Pchlde photoreduction. This latter process is catalyzed by the enzyme NADPH:Pchlde oxidoreductase (L-POR; E.C. 1.3.1.33) (see for a recent review Gabruk and Mysliwa-Kurdziel 2015).

The active site of L-POR has a strict geometry (Wilks and Timko 1995). The NADPH is arranged directly above the C17–C18 double bond of Pchlde, allowing a very fast electron (proton) transfer on illumination, leading to the saturation of this bond after getting the second proton (Lebedev and Timko 1999). As a consequence, Pchlde

✉ Béla Böddi
bela.boddi@gmail.com

¹ Department of Plant Anatomy, Institute of Biology, Eötvös Loránd University, Pázmány P. s. 1/c, Budapest 1117, Hungary

complexes containing NADP⁺ and lacking NADPH are not phototransformable, and the energy absorbed by Pchl_{ide} induces photooxidation and bleaching of Pchl_{ide} (Ryberg and Sundqvist 1988; Böddi and Franck 1997; Kirsch and de Groot 2001). On the other hand, the high ratio of NADPH/NADP⁺ was proved to inhibit Chl biosynthesis during greening (Zhang et al. 2014). Consequently, the normal biosynthesis of Chl-s needs an optimal NADPH/NADP⁺ ratio (Franck and Schmid 1985). The photoreduction results in the appearance of chlorophyllide (Chlide) complexes with emission maxima at 684 and 696 nm (Böddi et al. 1991), and as a result of Shibata shift (Shibata 1957) a 676–680 nm emitting chlorophyllide (Chlide) and/or Chl form accumulates (Domanskii and Rüdiger 2001).

Not all Pchl_{ide} is bound in the active site of L-POR. Various amounts of this pigment are present in other complexes, often mentioned as “free Pchl_{ide}” (El Hamouri et al. 1981). Besides Pchl_{ide}, protochlorophyll (Pchl), i.e., esterified Pchl_{ide}, is present in etiolated tissues, which is not a substrate of L-POR. The amounts of Pchl_{ide} and Pchl as well as their ratio are age, organ, and tissue dependent (Schoefs et al. 1994; Böddi et al. 2004). The excitation energy absorbed by these pigments cannot be used for their reduction; it is transferred mainly to molecular oxygen, thus reactive oxygen species (ROS) production is stimulated. Plant tissues abundant in free Pchl_{ide} and Pchl—for example the etiolated pea epicotyl (Böddi et al. 1994, 1998) and cabbage innermost leaves (Solymosi et al. 2004)—are thus light sensitive, i.e., their illumination leads to photodamage rather than to Chl biosynthesis (Erdei et al. 2005).

Despite the well-documented photosensitivity (Belyaeva and Litvin 2007), limited information is available about the photooxidation processes of etiolated tissues. The Pchl_{ide} content of etiolated tissues is significantly lower than the Chl content of green tissues, because Pchl_{ide} inhibits the synthesis of δ -aminolevulinic acid through a negative feedback mechanism (Richter et al. 2010). Under natural conditions, Pchl_{ide} is continuously reduced into Chlide which transforms into Chl-s and later Chl–protein complexes. This prevents the accumulation of photooxidation-sensibilizing pigments. Etiolated pea epicotyls contain short-wavelength Pchl_{ide} forms in great abundance (Böddi et al. 1994). These 629 and 636 nm emitting monomer forms (Böddi et al. 1998) were shown to act as sensibilizers of photooxidative damage processes, i.e., upon illumination, they transfer the absorbed energy to molecular oxygen and produce ROS (Erdei et al. 2005; Hideg et al. 2010). Epicotyls have a special pigment distribution basically different from that of etiolated leaves (Böddi et al. 1994); the latter ones are the usual experimental materials in works studying the photosynthetic apparatus. No detailed

analysis of photooxidation processes has been published about etiolated leaves. The inner leaves of cabbage deemed to be good research materials for studies on this question, since, similarly to pea epicotyls, monomer Pchl and Pchl_{ide} dominate in them. In addition, it has naturally developing etiolated tissue in great abundance, what is important in works, which require many samples. Cabbage heads are usually stored for long periods without observable breakdown processes, while leaves of etiolated seedlings show senescence and decomposition symptoms within two–three weeks.

Cabbage head is a modified bud containing internal etiolated leaf primordia and external fully green leaves. The tightly overlapping external leaf layers behave as optical filters and create a decreasing light gradient toward the center of the head (Solymosi et al. 2004). As a consequence of differently developed chloroplasts, Pchl_{ide} and Pchl are the dominating pigments in these leaves (Kruk 2005). These pigments were reported to be arranged into 629, 636, 644, and 655 nm emitting forms, according to the results of Gaussian deconvolution of 77 K fluorescence emission spectra (Solymosi et al. 2004). Interestingly, the analysis of the 77 K fluorescence emission spectra did not show the presence of the 633 nm form, reported earlier as a universal form in etiolated leaves (Böddi et al. 1992). This ambiguity indicates that further accurate analysis is needed to clarify the number and spectral properties of Pchl_{ide} forms in cabbage leaves. The 644 and 655 nm emitting forms also in cabbage leaves are L-POR-bound complexes since both transform into Chlide on flash illumination (Solymosi et al. 2004).

This work has been aimed at studying the wavelength dependence (i.e., the action spectra) of photoreduction and photooxidation processes and their ratio in innermost cabbage leaf pieces. The action spectrum, pigment content determination, and kinetic analyses confirmed that the excitation of the short-wavelength absorbing Pchl_{ide} form can cause photoreduction of the longer wavelength absorbing Pchl_{ide} forms at very low illumination intensities. However, at high actinic light intensities bleaching occurs.

Materials and methods

Plant material

Cabbage (*Brassica oleracea* var. *capitata* L.) heads were bought at the local market. The innermost leaves were dissected in darkroom at dim green light which was previously tested and did not cause Pchl_{ide} phototransformation. Freshly purchased and stored inner leaves were used in each experiment.

Fluorescence emission and excitation measurements

The room-temperature fluorescence spectra were measured with a Jobin–Yvon Horiba Fluoromax 3 (Paris, France) spectrofluorometer. When measuring emission spectra at room temperature, the PFD value of the excitation light was reduced to $0.02 \mu\text{mol photons m}^{-2} \text{s}^{-1}$ with neutral filters, and the change of the emission spectra was less than 1 % after three subsequent recordings. The emission spectra were measured in the 580–780 nm region with 0.5 nm data collection frequency, 0.1 s integration time, and 440 nm excitation light. The excitation and emission bandwidths were set to 2 and 5 nm, respectively. The emission spectra were corrected for the wavelength-dependent sensitivity variations of the spectrofluorometer.

The excitation spectra were corrected for the wavelength-dependent variations of the Xenon lamp emission. The spectra were recorded at 690, 710, and 730 nm emission wavelengths; the emission and excitation bandwidths were both set to 2 nm. A neutral filter was used to reduce the PFD values of the excitation light to around $0.02 \mu\text{mol photons m}^{-2} \text{s}^{-1}$.

Baseline correction and five-point linear smoothing were done using the SPSERV V.3.41. software (Copyright Cs. Bagyinka Biological Research Centre of the Hungarian Academy of Sciences). Using the same software, several spectra were resolved into Gaussian components in their wave number function, and then the results were re-converted into wavelength functions. A resolution was accepted when the error of the fit of the sum of Gaussians to the experimental spectrum was smaller than 1 %. To study the variability of the fluorescence emission intensities and band ratios, the AVEDEV (Excel function) spectrum of 90 “dark” spectra measured from 90 different innermost cabbage leaves was calculated according to Szenzenstein et al. (2008).

Kinetic measurements

In kinetic measurements, the excitation monochromator was set to 628, 638, or 650 nm with 2 nm bandwidth in each case (“actinic light”), while the emission monochromator was set to 680 nm with 5 nm bandwidth. The amplitude change of the 680 nm emission was recorded for 300 s with 0.5-s data collection interval and 0.5 s integration time.

Effects of 625–655 nm monochromatic actinic lights on the spectral properties of the leaves

A special experimental setup was applied to examine the effect of 625–655 nm monochromatic light on the spectral properties of inner leaves. After recording a “dark” spectrum using the neutral filter (see above), the excitation

monochromator was set to wavelengths between 625 and 655 nm with 2.5 nm steps, the neutral filter was removed, and the sample was illuminated with the monochromatic excitation light of the fluorometer for 300 s (using 2 nm excitation bandwidth). To compare the effects of actinic lights with different wavelengths, the amplitude values of emission spectra measured after irradiation were normalized to $7 \mu\text{mol photons m}^{-2} \text{s}^{-1}$. In some experiments, the PFD value of the actinic light was reduced to $0.7 \mu\text{mol photons m}^{-2} \text{s}^{-1}$ with a neutral filter.

Measurement of the absorption spectra

The absorption spectra were recorded with a Shimadzu UV-2101 PC spectrophotometer (Shimadzu Corp., Kyoto, Japan), in the 600–700 nm region. The data were collected with 0.5 nm frequency, and the optical slit was 1 nm. The mean of five spectra recorded from different segments of the same leaf was calculated and used for further analysis.

Measurements under oxygen-reduced and oxygen-enriched atmospheres

A 5 mm × 20 mm leaf piece was fixed in a 1-cm-diameter test tube equipped with vacuum connection adapter. After recording a “dark” spectrum, the test tube was connected to a vacuum water pump for 10 min and then to a nitrogen-containing balloon to obtain oxygen-reduced environment with ambient pressure. The sample was incubated in the dark for 30 min, and the fluorescence emission spectrum was recorded again. The sample was illuminated with 628 nm actinic light of $5 \mu\text{mol photons m}^{-2} \text{s}^{-1}$ for 300 s as described above, and then replacing the neutral filter the emission spectrum was recorded again. In another experiment, this test tube was connected to an oxygen balloon and the ambient air was enriched with oxygen. The leaf sample was kept in this environment for 15 min, and the same measurements were done as above. In both cases, control experiments were run with same experimental setup but in ambient environment.

Measuring regeneration of the protochlorophyllide forms

Emission spectra of dark and 628 nm actinic light-illuminated samples were recorded as described above. The samples were kept in dark for 1 min, 30 min, 1, 2, 4, 6, 12, 24, 48, and 72 h in a thin plastic foil. After each dark period, the emission spectrum was recorded. Since the leaf piece was fixed in the sample holder, all spectra were recorded exactly from the same spot of the leaf. This procedure was repeated with three leaf pieces, but the representative results measured from one leaf are shown.

Statistical methods

We conducted the statistical evaluation of results using Microsoft Excel 2010 and SPSS V. 17.0 software (Copyright Cs. Bagyinka Biological Research Centre of the Hungarian Academy of Sciences) spectrum analytical program. We calculated average and AVEDEV spectra using Excel. The AVEDEV spectrum shows which emission bands are standard and which ones vary in their intensity or position (Szenzenstein et al. 2008). In some cases, we calculated the standard deviation (SD) of specific data points (emission maximum and minimum) of average spectra and used SD values to evaluate the reliability of the results.

Pigment determination

Dark samples or the illuminated spots of leaves were dissected, their fresh mass values were measured, and the pigments were extracted with acetone. The fluorescence emission spectra were recorded with 430 nm excitation. A calibration curve was used for the concentration calculations (Vitányi et al. 2013). The mean and standard error values of three parallels were calculated.

Results

Room-temperature fluorescence and absorption properties of the innermost leaves of cabbage

To study the photosensitivity of pigment forms, it is crucial to study the room-temperature emission spectrum and the number and ratio of spectral components. In this work, the emission spectra of 90 leaf pieces were measured at room temperature, the mean spectrum of which was calculated and resolved into Gaussian components which were found at 633.2, 643.5, 655.1, 668.0, 680.0, 692.3, 713.2, and 735.1 nm (Fig. 1).

To measure the variability of spectral components (amplitude and position of different emission bands) in the dark samples, the AVEDEV spectrum was calculated. A sharp and symmetrical band appeared with maximum at 641.5 nm, the amplitude of which was around 15 % of the maximum of the average spectrum. In addition, a smaller band was found at 678.0 nm (Fig. 1, inset).

To get information about the effective wavelength values for further irradiation experiments, the absorption spectra of the inner leaves were recorded. The mean spectrum of 5 leaf pieces had an absorption maximum at 632 nm (Fig. 2). The Gaussian resolution of the absorption spectrum showed overlapping components at 628.6, 638.2, and 652.0 nm (and a broad, low-intensity band with

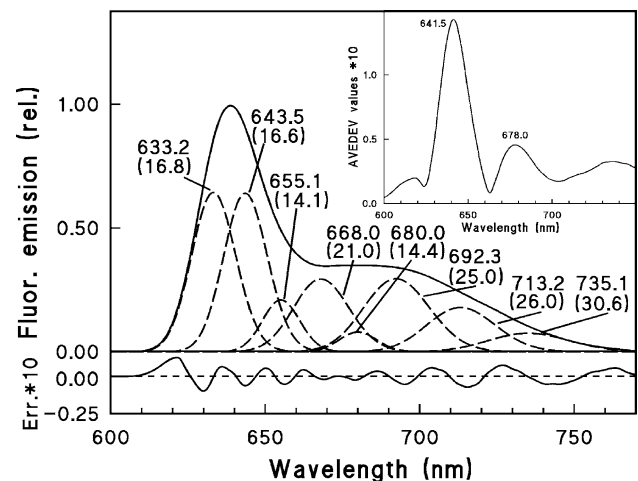


Fig. 1 Average of 90 room-temperature fluorescence emission spectra measured from 90 inner leaf samples (*solid line*) and the Gaussian components (*broken lines*). The maximum positions and half-bandwidth values (in parenthesis) are indicated above the components in nm. The excitation wavelength was 440 nm and the spectra were normalized to their total integral. *Inset* shows the AVEDEV spectrum of the 90 spectra

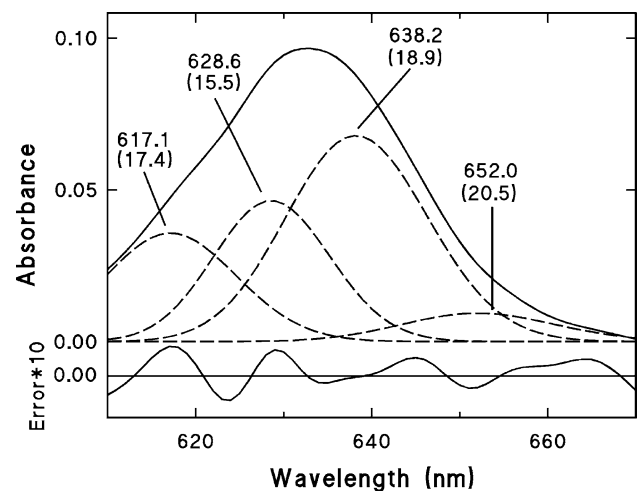


Fig. 2 Absorption spectrum of cabbage innermost leaf in the red region. *Solid line* the mean spectrum of 5 innermost cabbage leaf pieces in the red region. *Dashed lines* the Gaussian components corresponding to the protochlorophyllide forms. The maximum positions and the half-bandwidth values (in parentheses) are given in nm

maximum at 617.1 nm was identified; since it must be a $Q_x(0-0)$ transition overlapped with vibronic satellite $Q_y(0-1)$ band, we do not discuss it in this paper.)

To achieve accurate interpretation of the absorption bands, the room-temperature excitation spectra were recorded with the emission monochromator set to 690, 710, or 730 nm (which correspond to the vibronic satellite bands of the 633, 644, and 655 nm emitting Pchl_a forms, respectively (Böddi et al. 1992)). These spectra clearly

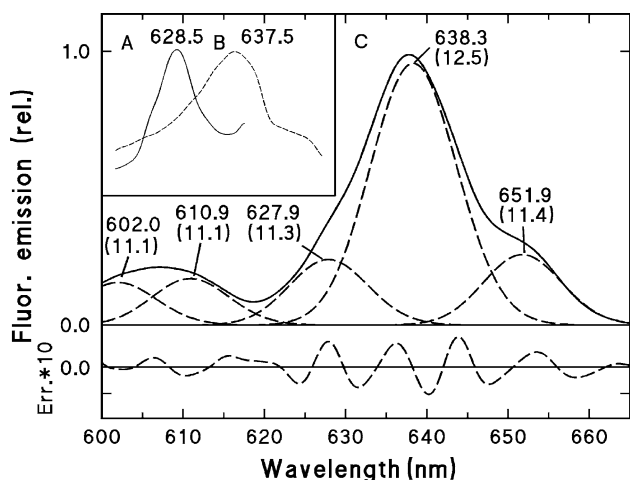


Fig. 3 Room-temperature excitation spectra of inner leaves of white cabbage measured at 690 (A), 710 (B), and 730 nm (C) emission wavelengths. The Gaussian components with their maxima and half-bandwidth values (in parentheses) are given in nm (C, dashed lines). The fitting error of the Gaussian deconvolution was smaller than 1 % (bottom panel, dashed line)

showed the existence of excitation bands at 628–628.5, 637.5–638.5, and at around 652 nm (Fig. 3). The excitation spectrum measured at 730 nm emission was resolved into Gaussian components; this analysis showed components at 602.0 and 610.9 nm which are probably Q_x transitions (Houssier and Sauer 1970) or vibrational satellite bands of different protochlorophyllide forms (Böddi et al. 1998). Other components were detected at 627.9, 638.3, and 651.9 nm (Fig. 3C, dashed lines).

The effect of natural sunlight

To test their light sensitivity, innermost leaves were illuminated with natural sunlight of $3000 \mu\text{mol photons m}^{-2} \text{s}^{-1}$ PFD for 5 min. A significant decrease of the 638.5 nm fluorescence signal was observed, and only a small increase of a 676 nm emission band was found (Fig. 4).

The difference spectrum, calculated via subtracting the spectrum of the non-illuminated sample from that of the illuminated, had a strong, blue-shifted (to 637.5 nm) negative band and a little positive signal at around 680 nm (Fig. 4 inset). The changes in the pigment contents corresponded to these spectroscopic observations; while the Pchl(ide) content of the non-illuminated leaves was $(33 \pm 2.0) \times 10^{-5} \mu\text{M g}^{-1}$ fresh mass, this value decreased to $(1.8 \pm 1.3) \times 10^{-5} \mu\text{M g}^{-1}$ fresh mass in the illuminated leaves (i.e., around 20 times smaller value). On the other hand, the Chl(ide) content was $(3.7 \pm 1.5) \times 10^{-5} \mu\text{M g}^{-1}$ fresh mass in the dark samples, and the irradiation resulted in only a slight increase to $(7.7 \pm 1.8) \times 10^{-5} \mu\text{M g}^{-1}$ fresh mass.

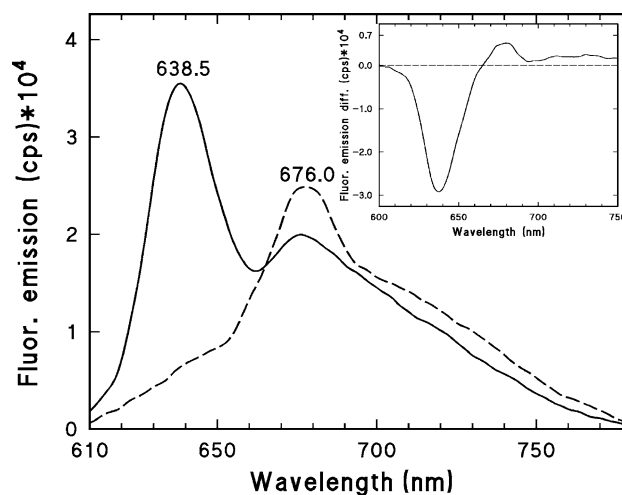


Fig. 4 The effect of sunlight on cabbage innermost leaves. Room-temperature fluorescence emission spectrum before (solid line) and after 5-min illumination (dashed line). The excitation light was set to 440 nm. Inset shows the difference spectra of illuminated and dark leaves of cabbage. The PFD of the sunlight was $3000 \mu\text{mol photons m}^{-2} \text{s}^{-1}$

Irradiation with monochromatic light

The drastic decrease in the Pchl(ide) content and the small increase in the Chl(ide) content in the cabbage leaves indicated that at least two parallel processes took place upon irradiation with sunlight, i.e., strong bleaching of Pchl and Pchl(ide) and minor photoreduction of Pchl(ide) occurred. To study the details of these reactions, the inner leaves were illuminated with monochromatic actinic light varying the wavelength between 625 and 655 nm with 2.5 nm steps. The irradiation period was 300 s since a preliminary experiment showed that the amplitude decrease of the fluorescence emission signal reached a standard value, i.e., it saturated at around 300-s irradiation.

Considering the heterogeneity of the dark samples, the difference spectra of the “illuminated” and “dark” (illuminated minus dark) spectra were calculated for each experiment with various actinic lights. The negative bands showed the transformed or bleached Pchl(ide), and the positive signals indicated Chl(ide) formation. The difference spectra were corrected for the Xenon lamp profile, and then they were collected into a database. The 3D surface and its topological projection were calculated. A well-distinguishable minimum was found at 639.7 nm and at 642.5 nm actinic light, while a little, non-significant increase was found at 678 nm in the emission difference when the wavelength of the actinic light was 652 nm (Fig. 5; X and Y points, respectively).

The sections of the 3D image at 633, 644, 655, and 680 nm emission values show the action spectra of the spectral changes of Pchl(ide) and Chl(ide) forms,

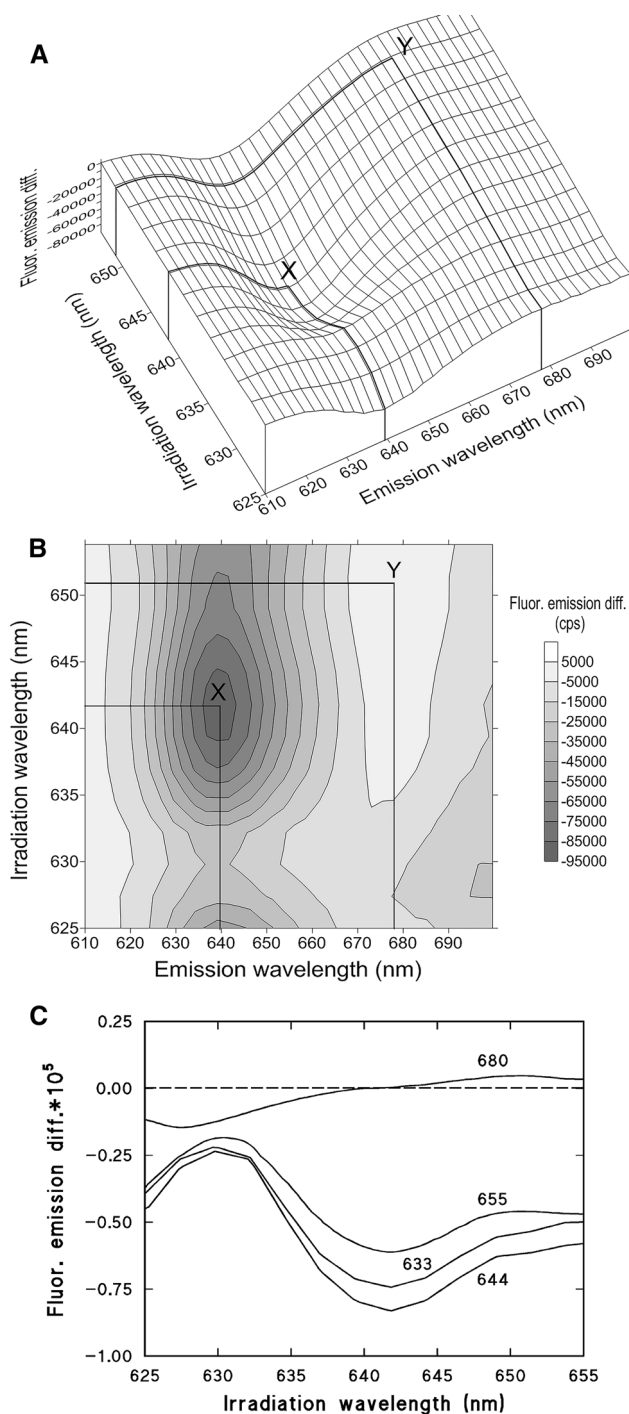


Fig. 5 The effect of 625–655 nm monochromatic light of $7 \mu\text{mol photons m}^{-2}\text{s}^{-1}$ PFD for 300 s on cabbage inner leaves. The illuminated minus dark spectra were collected into a database to calculate the 3D image of the spectral changes (**A**) and its topological projection (**B**). The thickened contours indicate the minimum at the intersection of 639.7 and 642.5 nm (*X*) and the maximum at the intersection of 678 and 652 nm (*Y*) values. The (**C**) panel shows the sections of the 3D image, i.e., action spectra, of the spectral changes of Pchl(ide) and Chl(ide) forms emitting at 633, 644, 655, and 680 nm emission wavelength values. The difference spectra were corrected for the Xenon lamp profile

indicating the sum of photooxidation and photoreduction processes. Interestingly, the actinic light (i.e., irradiation wavelength) at around 630 nm caused a smaller fluorescence decrease than the 638–642.5 nm light in the 633, 644, and 655 nm emission amplitude values. (It should be mentioned, that the difference spectra showed a moderate variability in their minimum values, varying in the 638–642.5 nm wavelength interval.) The action spectrum at 680 nm had minimum values under 640 nm, had a zero-crossing at 638–641 nm, and was positive at longer wavelengths (Fig. 5C).

Kinetic measurements of the fluorescence emission at 680 nm during 5-min irradiation with 628, 638, or 650 nm actinic lights

During the irradiation of the samples with various wavelengths of actinic light, the fluorescence emission changes were recorded in kinetics mode of the fluorometer with the emission monochromator set to 680 nm. The results of three, 628, 638, and 650 nm, irradiation experiments were analyzed in detail because the absorption and fluorescence excitation spectra of the dark leaves showed absorption/excitation bands in these positions (Figs. 2 and 3).

The 628 nm irradiation resulted in an initial amplitude increase in the first approximately 1 min, then a significant signal decrease took place; the amplitude value became zero at 250 s and then became negative. A faster amplitude increase was found at 638 nm irradiation; its maximum was around 40 s. The slope of the kinetic curve was less pronounced than at 628 nm irradiation; it reached a nearly constant value of above 250 s. The amplitude of the emission was higher than the initial value, indicating Chlide and Chl synthesis. A continuous increase of the 680 nm emission amplitude took place at 650 nm irradiation; the value at 300 s was significantly higher than the initial value (Fig. 6).

The pigment determination results were in good agreement with the action spectra and the fluorescence kinetic measurements. At 628 nm irradiation, the Pchl(ide) content remarkably decreased and the Chl(ide) content also decreased. At 638 nm irradiation, the Pchl(ide) content decreased to a lesser extent than at 628 nm actinic light, and the Chl(ide) content increased compared to the Chl(ide) content of dark leaves. The 650 nm irradiation resulted in only a slight decrease in the Pchl(ide) content, while the Chl(ide) content almost doubled (Table 1).

We observed that bleaching became stronger, if the cabbage heads were stored for 14 days and the fluorescence amplitude values of the dark samples decreased to about 70 % compared to those of the freshly purchased ones. These inner leaves were illuminated with 628, 638, and

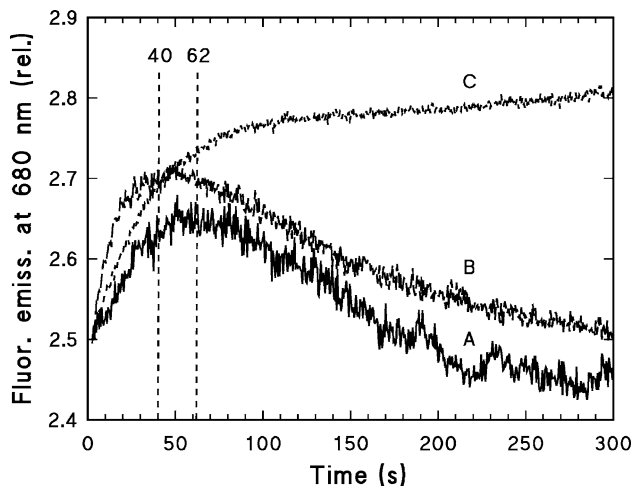


Fig. 6 The changes of 680 nm fluorescence emission amplitude values during illumination with 628 (A), 638 (B), or 650 (C) nm monochromatic light. The amplitude values were corrected for the wavelength-dependent intensity variation of the excitation light of the Xenon lamp, i.e., normalized for $7 \mu\text{mol photons m}^{-2} \text{s}^{-1}$ PFD value. The amplitude values were normalized for the mean dark value at 680 nm emission wavelength. The estimated maxima of the 680 nm intensity changes are indicated by broken lines

650 nm monochromatic light for 300 s using exactly the same experimental setup applied as before. The relative amplitude of the 680 nm emission decreased continuously in the case of 628 nm illumination. Unlike freshly purchased leaves (Fig. 6A), no initial increase but a gradual decrease of the relative amplitude were observed (Fig. 7A). 638 nm caused a smooth increase of relative amplitude in the first approximately 60 s of illumination, and only a moderate decrease happened during the further illumination. The final amplitude value remained higher compared to the case of fresh cabbage leaves (Fig. 7). Finally, 650 nm illumination generated slow and continuous increase of the 680 nm amplitude in the first 60 s of illumination and remained approximately stable, but the increase was smaller than seen in the case of fresh leaves (Fig. 7).

The initial amplitude increase of the 680 nm emission signal brought up the possibility that this light might cause phototransformation of Pchl_{id} forms absorbing at longer

wavelengths. To study this phenomenon, leaves from a cabbage head stored for 2 weeks were illuminated with 628 nm light of $0.7 \mu\text{mol photons m}^{-2} \text{s}^{-1}$ PFD value for 300 s. This illumination caused only a minimal decrease of the 640 nm band; in the “illuminated minus non-illuminated” difference spectrum, this decrease was $-19.67 \pm 6.43 \%$ of the amplitude of the non-illuminated sample. In parallel, a positive band appeared at 678 nm. Interestingly, the amplitude value at 680 nm continuously increased during the illumination (Fig. 8), and the kinetic curve was similar to the one observed at 650 nm illumination of $7 \mu\text{mol photons m}^{-2} \text{s}^{-1}$ (Figs. 6 and 7).

The effects of oxygen-reduced or oxygen-enriched environments on the extent of irradiation-caused spectral changes

In the case of cabbage that was stored for 14 days, the oxygen-reduced environment decreased the extent of spectral changes (Fig. 9). When the oxygen content was low during the 628 nm irradiation, the decrease of the 639 nm band was $59.11 \pm 3.25 \%$ taking to 100 % of the amplitude of the same band in the spectrum of the non-illuminated sample. In case of control, the extent of the decrease was $67.78 \pm 6.37 \%$.

This latter value is not comparable with the above-described results because the illumination conditions were different. In this experiment, the curvature of the glass sample holder test tube caused scattering reducing the PFD value of the actinic light. To get similar PFD value as in the experiments above, the slit of the actinic light was set to 3 nm.

When the leaves were kept in oxygen-enriched environment during the 628 nm irradiation, no significant difference was found compared to the ambient air conditions (not shown).

Regeneration of protochlorophyllide forms

To test the regeneration ability of the irradiated leaves that were stored only 1 day after purchase, an inner leaf piece

Table 1 Changes in the pigment contents of innermost leaves of cabbage upon irradiation with light of different wavelengths of $7 \mu\text{mol photons m}^{-2} \text{s}^{-1}$ PFD (corrected with the wavelength-dependent intensity variations of the Xenon lamp of the spectrofluorometer) for 300 min. ($n = 3$)

Irrad. (nm)	Pchl(id) ($\mu\text{mol g}^{-1} \text{f.m.}) \times 10^{-5}$)	Pchl(id)-illuminated minus dark ($\mu\text{mol g}^{-1} \text{f.m.}) \times 10^{-5}$)	STD ($\mu\text{mol g}^{-1} \text{f.m.}) \times 10^{-5}$)	Chl(id) ($\mu\text{mol g}^{-1} \text{f.m.}) \times 10^{-5}$)	Chl(id)-illuminated minus dark ($\mu\text{mol g}^{-1} \text{f.m.}) \times 10^{-5}$)	STD ($\mu\text{mol g}^{-1} \text{f.m.}) \times 10^{-5}$)
Dark	33.2	–	2.0	3.7	–	1.5
628	7.3	–25.9	3.0	2.2	–1.5	0.2
638	10.7	–22.5	2.5	4.2	0.5	0.8
650	26.9	–6.3	7.2	7.4	3.7	1.0

fm fresh mass, *STD* standard deviation, *Irrad.* irradiation

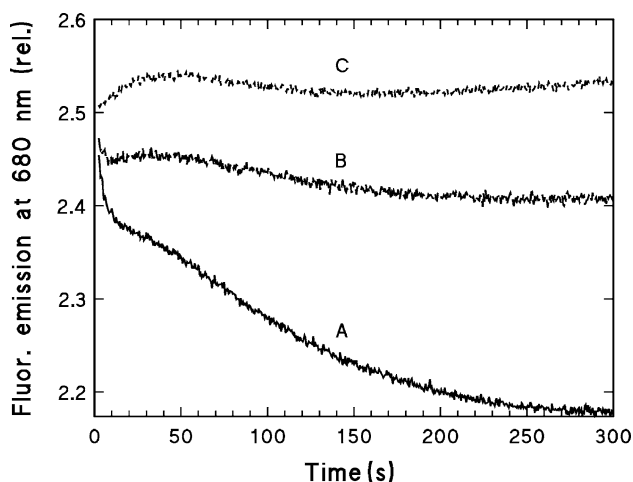


Fig. 7 The effect of 300 s monochromatic illumination on leaves stored for 14 days after purchase. The changes of 680 nm fluorescence emission amplitude values during illumination with 628 (A curve), 638 (B curve), or 650 nm (C curve) monochromatic light. The amplitude values were corrected for the wavelength-dependent intensity variation of the excitation light of the Xenon lamp. The amplitude values were normalized for the mean dark value at 680 nm emission wavelength, and the measurements were done using cabbage stored for 14 days after purchase

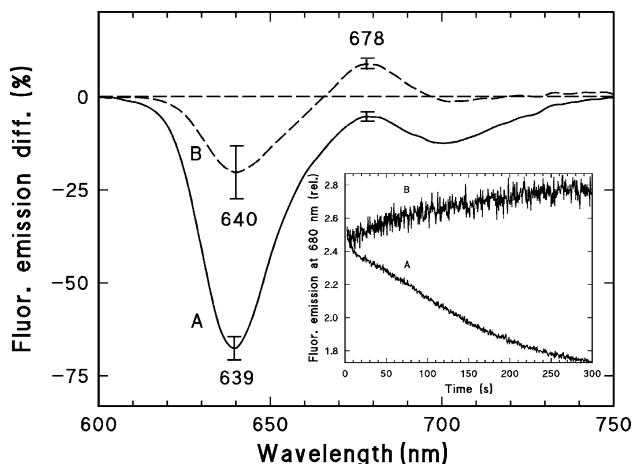


Fig. 8 Average difference spectra ($n = 5$) of samples irradiated with 628 nm monochromatic light of $7 \mu\text{mol photons m}^{-2} \text{s}^{-1}$ PFD value (solid line) and $0.7 \mu\text{mol photons m}^{-2} \text{s}^{-1}$ PFD value (dashed line) for 300 s. The amplitude values were corrected for the wavelength-dependent intensity variation of the excitation light of the Xenon lamp, i.e., normalized for $7 \mu\text{mol photons m}^{-2} \text{s}^{-1}$ PFD value, and the amplitude values were normalized for the amplitude of the dark spectrum at 680 nm emission wavelength. Standard deviation of the emission difference values at 639–641 and 678 nm emission is indicated by scaled bars. (100 % is the amplitude of the spectrum of the leaf before illumination.) Inset shows the changes of 680 nm fluorescence emission amplitude values during illumination with 628 nm monochromatic light of $7 \mu\text{mol photons m}^{-2} \text{s}^{-1}$ PFD value (A) and $0.7 \mu\text{mol photons m}^{-2} \text{s}^{-1}$ PFD value (B) for 300 s. The amplitude values were normalized for the mean dark value at 680 nm emission wavelength

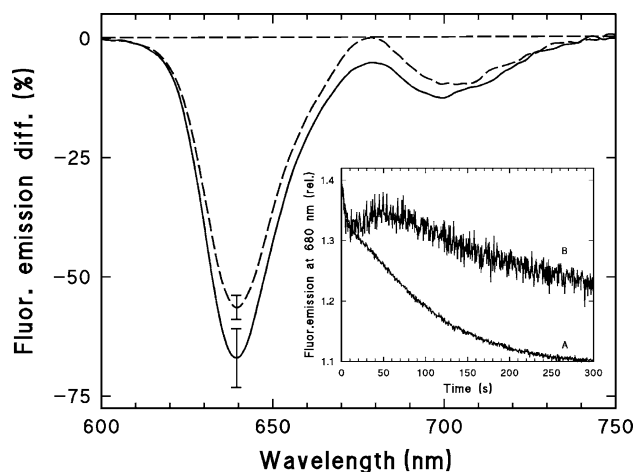


Fig. 9 Average difference spectra ($n = 5$) of samples irradiated with 628 nm monochromatic light of $7 \mu\text{mol photons m}^{-2} \text{s}^{-1}$ PFD value in oxygen-reduced and N_2 -enriched (dashed line) and ambient atmosphere (solid line) for 300 s. Standard deviation of the emission difference values at 639 nm emission is indicated by error bars. (100 % is the amplitude of the spectrum of the leaf before illumination.) Inset shows the changes of 680 nm fluorescence emission amplitude values during illumination with 628 nm monochromatic light in oxygen-reduced (B) and ambient (A) atmospheres. The amplitude values were corrected for the wavelength-dependent intensity variation of the excitation light of the Xenon lamp, i.e., normalized for $7 \mu\text{mol photons m}^{-2} \text{s}^{-1}$ PFD value. The amplitude values were normalized for the dark value at 680 nm emission wavelength

(wrapped into plastic foil to avoid water loss) was illuminated with 628 nm of $7 \mu\text{mol photons m}^{-2} \text{s}^{-1}$ PFD for 5 min, the fluorescence emission spectrum was recorded, and the sample was kept in the dark for 72 h. After different time periods, fluorescence emission spectra were measured. The emission maximum of the “dark” spectrum was at 638 nm, and the spectrum had broad vibronic satellite bands above 670 nm (Fig. 10A, dashed curve). The irradiation caused a significant decrease of the Pchl_a band; in parallel, it shifted to 634.5–635 nm and an independent band appeared at 677–679 nm (Fig. 10B, curve). In the first 4 h of dark incubation, the intensity of the emission spectrum did not change considerably. During 6 h of dark incubation, the amplitude of the 634.5–635 nm band increased (Fig. 10C, curve), then after 24 h this band showed further increase and its position shifted back to 637 nm (Fig. 10D, curve). The increase of the 637–638 nm band proceeded (Fig. 10E, curve); after 72 h dark incubation, its amplitude was almost identical to that of the dark sample (Fig. 10F, curve). During the 72 h dark incubation, the amplitude of the 677–679 nm band changed only slightly.

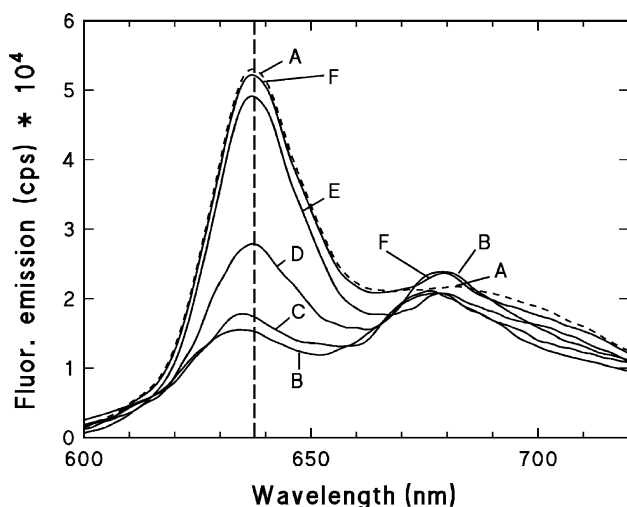


Fig. 10 Regeneration of Pchl_{ide} forms in cabbage inner leaves incubated in the dark after 5-min irradiation with 628 nm of $7 \mu\text{mol photons m}^{-2} \text{ s}^{-1}$ PFD. **A** The spectrum of the leaf before the irradiation; **B** the spectrum measured directly after the irradiation; **C–F** the spectra recorded after 6-, 24-, 48-, and 72-h dark incubation, respectively. The vertical line shows the original emission maximum at 638 nm

Discussion

The increased light sensitivity of etiolated tissues is a well-known phenomenon; light causes wilting and damage of dark-grown plants. Detailed analysis of the irradiation-caused reactions showed that besides the photoreduction of L-POR-connected Pchl_{ide} molecules into Chlide, photooxidation reactions are provoked (Erdei et al. 2005). The produced ROS were identified in epicotyls of dark-germinated pea in which the short-wavelength, monomer Pchl_{ide} forms dominate (Hideg et al. 2010). Similarly to the etiolated pea epicotyls, the short-wavelength Pchl_{ide} forms are abundant in innermost leaves of cabbage (Solymosi et al. 2004), thus the question can be raised if these chromophores provoke similar photooxidation.

To identify the sensibiliser of the photooxidation, the measurement of the action spectrum is a suitable method. Because of the low pigment content of cabbage leaves, fluorescence spectroscopy is a proper tool; however, the measurement of room-temperature spectra of light-sensitive samples is difficult (Böddi and Franck 1997). The experimental setup (the strong neutral filter in the excitation beam) used in this work allowed us to record spectra from the same leaf spot before and after irradiation. On the other hand, the PFD value of the direct excitation light of the fluorometer was big enough to provoke pigment bleaching in the innermost leaves. After correcting the amplitude values for the emission profile of the Xenon lamp, the extent of bleaching caused by different wavelengths of the actinic

lights could be compared with each other, i.e., action spectra could be measured.

The room-temperature fluorescence spectra of cabbage leaves had low amplitude and were less structured than the 77 K spectra (Solymosi et al. 2004). The analyses of the absorption (Fig. 2), fluorescence emission (Fig. 1), and excitation spectra (Fig. 3) led us to assume that the changes of three Pchl_{ide} forms with emission maxima at around 633, 644, and 655 nm should be followed. The analyses of the spectra measured at room temperature in this work showed that the presence of the additional 636 nm form (Solymosi et al. 2004) is not necessary to get a fit with less than 1 % error, and the resolutions of the absorption, fluorescence excitation, and emission spectra into Gaussian components gave steadily similar results.

Important information can be obtained about the effects of illumination by the measurement of the fluorescence emission intensity changes at 680 nm during the illumination. This intensity change (Figs. 6 and 7) is a resultant of the decreasing amplitude of the vibronic satellite band of the 633 nm emitting Pchl_{ide} form (Böddi et al. 1992) and of the alteration of the emission amplitude of Chlide (Böddi and Franck 1997). The 680 nm emission signal increases as a result of Pchl_{ide} photoreduction into Chlide; however, it can decrease due to bleaching of monomer Pchl_{ide} and/or Chlide. In addition, the fluorescence yields of Pchl_{ide} and Chlide are different, and therefore the amplitude change of the 680 nm fluorescence band does not show stoichiometric amounts of Chlide but allows qualitative conclusions about the ratio of pigment formation or bleaching.

The action spectrum of the fluorescence amplitude change at 680 nm (Fig. 6) crosses the zero line between 638 and 642 nm. This indicates that the actinic light of low ($7 \mu\text{mol photons m}^{-2} \text{ s}^{-1}$) PFD does not cause strong bleaching above 638 nm. Even more, the 638 nm actinic light is more effective in the excitation of the 655 nm Pchl_{ide} form than the 650 nm actinic light. This is proven by the highest amplitude band at 638.3 nm in the excitation spectrum measured at 730 nm (Fig. 3C, which is the emission maximum of the vibronic satellite band of the 655 nm Pchl_{ide} form (Böddi et al. 1992). Also the steeper rise of the kinetic curve measured at 638 nm than at 650 nm actinic light in the first 40 s (Fig. 6) confirms the high quantum efficiency of 638 nm light in Chlide formation. Taking into account the high abundance of 644 nm Pchl_{ide} in cabbage leaves and the fact that this form is a very effective energy donor of 655 nm Pchl_{ide} form (Kahn et al. 1970), we can assume that the 638 nm light excites more phototransformable Pchl_{ide} simultaneously than the 650 nm actinic light.

In contrast with the 638 and 650 nm actinic lights, the 628 nm illumination can induce both photoreduction and

bleaching, depending on its PFD value and the physiological state (fresh or stored) of the cabbage leaves. Illumination of fresh leaves induces photoreduction in the first 60 s at 7 $\mu\text{mol photons m}^{-2} \text{s}^{-1}$ PFD, and subsequently bleaching proceeds (Fig. 6). In the case of stored leaves, continuous amplitude decline at 680 nm (i.e., strong bleaching) was observed from the onset of illumination (Fig. 7A). Surprisingly, steady photoreduction took place if the PFD value of the 628 nm actinic light was reduced to an extremely low value (0.7 $\mu\text{mol photons m}^{-2} \text{s}^{-1}$) (Fig. 8). As a summary, photoreduction saturates at a low PFD compared to bleaching, suggesting that the quantum yield of photoreduction is higher than that of bleaching.

Bleaching sensitized by free tetrapyrroles is well known (Busch and Montgomery 2015). Such a sensitizer can be for example non-L-POR-bound Pchl(ide) in pea epicotyl (Erdei et al. 2005) and the short-wavelength emitting Pchl(ide) forms in the flu mutant of *Arabidopsis* (Meskauskiene et al. 2001, op den Camp et al. 2003). This work provides direct evidence that also the 633 nm emitting Pchl(ide) form can provoke photooxidation in 628 nm illuminated cabbage leaves. The extent of bleaching could be reduced by decreasing the oxygen content in the direct environment of the samples (Fig. 9) suggesting the involvement of ROS in this process. The bleaching observed during 628 nm illumination was the result mainly of Pchl(ide) but also Chlide destruction (Table 1), and the long (72 h) regeneration period (Fig. 10) supports further this assumption. The bleaching of Chlide can be caused partly by the actinic light but indirectly by the reaction with ROS molecules produced by the excitation of the non-photoreducible Pchl(ide) molecules. The length of the regeneration time indicates that obviously de novo biosynthesis processes took place.

Interestingly, the 628 nm light of very low PFD (0.7 $\mu\text{mol photons m}^{-2} \text{s}^{-1}$) did cause photoreduction without observable bleaching (Fig. 8). This light excites the 633 nm emitting Pchl(ide) form which is not directly photoactive even with 632.8 nm laser illumination (Kósa and Böddi 2012). Consequently, the photoreduction of longer wavelength Pchl(ide) forms took place which could proceed via energy migration (Franck et al. 2000). An alternative energy source for the phototransformation of longer wavelength Pchl(ide) forms is the 633 nm light emitted by the non-photoactive Pchl(ide) molecules, i.e., reabsorption proceeds.

These findings confirm that the abundance of the monomer state of Pchl(ide) pigment can be the reason of photooxidation in etiolated cabbage leaves, but its excitation energy can reach the longer wavelength, photoactive Pchl(ide)-L-POR complexes via excitation transfer, or fluorescence reabsorption and can stimulate Pchl(ide) photoreduction into Chlide.

Acknowledgments We are grateful to the following former students for their contribution in data collection: Katia Plouznikoff, master student of Université de Bourgogne, Dijon, France; also Valeria Ketykó and Dénes Kleiner undergraduate students of Semmelweis University Budapest, Hungary.

References

- Belyaeva OB, Litvin FF (2007) Photoactive pigment-enzyme complexes of chlorophyll precursor in plant leaves. *Biochemistry (Moscow)* 72:1458–1477
- Böddi B, Franck F (1997) Room temperature fluorescence spectra of protochlorophyllide and chlorophyllide forms in etiolated bean leaves. *J Photoch Photobiol B* 41:73–82
- Böddi B, Ryberg M, Sundqvist C (1991) The formation of a short-wavelength chlorophyllide form at partial phototransformation of protochlorophyllide in etioplast inner membranes. *Photochem Photobiol B* 53:667–673
- Böddi B, Ryberg M, Sundqvist C (1992) Identification of four universal protochlorophyllide forms in dark-grown leaves by analyses of the 77 K fluorescence emission spectra. *J Photoch Photobiol B* 12:389–401
- Böddi B, Mc Ewen B, Ryberg M, Sundqvist C (1994) Protochlorophyllide forms in non-greening epicotyls of dark-grown pea (*Pisum sativum*). *Physiol Plant* 92:160–170
- Böddi B, Kis-Petik K, Kaposi AD, Fidy J, Sundqvist C (1998) The two spectroscopically different short wavelength protochlorophyllide forms in pea epicotyls are both monomeric. *Biochim Biophys Acta* 1365:531–540
- Böddi B, Bóka K, Sundqvist C (2004) Tissue specific protochlorophyll (ide) forms in dark-forced shoots of grapevine (*Vitis vinifera* L.). *Photosynth Res* 82:141–150
- Busch AW, Montgomery BL (2015) Interdependence of tetrapyrrole metabolism, the generation of oxidative stress and the mitigative oxidative stress response. *Redox Biol* 4:260–271
- Domanskii VP, Rüdiger W (2001) On the nature of the two pathways in chlorophyll formation from protochlorophyllide. *Photosynth Res* 68:131–139
- El Hamouri B, Brouers M, Sironval C (1981) Pathway from photoinactive p 633–628 protochlorophyllide to the p 696–682 chlorophyllide in cucumber etioplast suspension. *Plant Sci Lett* 21:375–379
- Erdei N, Cs Barta, Hideg E, Böddi B (2005) Light-induced wilting and its molecular mechanism in epicotyls of dark-germinated pea (*Pisum sativum* L.) seedlings. *Plant Cell Physiol* 46:185–191
- Franck F, Schmid GH (1985) The role of NADPH in the reversible phototransformation of chlorophyllide P682 into chlorophyllide P678 in etioplasts of oat. *Z Naturforsch C* 40:832–838
- Franck F, Sperling U, Frick G, Pochert B, van Cleve B, Apel K, Armstrong GA (2000) Regulation of etioplast pigment-protein complexes, inner membrane architecture, and protochlorophyllide a chemical heterogeneity by light-dependent NADPH: protochlorophyllide oxidoreductases A and B. *Plant Phys* 124(4):1678–1696
- Gabruk M, Mysliwa-Kurziel BJ (2015) Light-dependent protochlorophyllide oxidoreductase: phylogeny, regulation and catalytic properties. *Biochemistry-US*. doi:10.1021/acs.biochem.5b00704
- Hideg É, Vitányi B, Kósa A, Solymosi K, Bóka K, Won S, Inoue Y, Ridge R, Böddi B (2010) Reactive oxygen species from type-I photosensitized reactions contribute to the light-induced wilting of dark-grown pea (*Pisum sativum*) epicotyls. *Physiol Plantarum* 138:485–492
- Houssier C, Sauer K (1970) Circular dichroism and magnetic circular dichroism of the chlorophyll and protochlorophyll pigments. *J Am Chem Soc* 92:779–791

- Kahn A, Boardman NK, Thorne SW (1970) Energy transfer between protochlorophyllide molecules: evidence for multiple chromophores in the photoactive protochlorophyllide-protein complex in vivo and in vitro. *J Mol Biol* 48:85–101
- Kirsch M, de Groot H (2001) NAD(P)H, a directly operating antioxidant? *FASEB J* 15:1569–1574
- Kósa A, Böddi B (2012) Dominance of a 675 nm chlorophyll(ide) form upon selective 632.8 or 654 nm laser illumination after partial protochlorophyllide phototransformation. *Photosynth Res* 114:111–120
- Kruk J (2005) Occurrence of chlorophyll precursors in leaves of cabbage heads—the case of natural etiolation. *J Photoch Photobio B* 80:187–194
- Lebedev N, Timko M (1999) Protochlorophyllide oxidoreductase B-catalyzed protochlorophyllide photoreduction in vitro: insight into the mechanism of chlorophyll formation in light-adapted plants. *P Natl Acad Sci USA* 96:9954–9959
- Meskauskiene R, Nater M, Goslings D, Kessler F, op den Camp R, Apel K (2001) FLU: a negative regulator of chlorophyll biosynthesis in *Arabidopsis thaliana*. *P Natl Acad Sci USA* 98:12826–12831
- op den Camp RG, Przybyla D, Oehsenbein C, Laloi C, Kim C, Danon A, Wagner D, Hideg É, Göbel C, Feussner I, Nater M, Apel K (2003) Rapid induction of distinct stress responses after the release of singlet oxygen in *Arabidopsis*. *Plant Cell* 15:2320–2332
- Richter A, Peter E, Pörs Y, Lorenzen S, Grimm B, Czarnecki O (2010) Rapid dark repression of 5-aminolevulinic acid synthesis in green barley leaves. *Plant Cell Physiol* 51:670–681
- Ryberg M, Sundqvist C (1988) The regular ultrastructure of isolated prolamellar bodies depends on the presence of membrane-bound NADPH-protochlorophyllide oxidoreductase. *Physiol Plant* 73:18–226
- Schoefs B, Garnir HP, Bertrand M (1994) Comparison of the photoreduction of protochlorophyllide to chlorophyllide in leaves and cotyledons from dark-grown bean as a function of age. *Photosynth Res* 41:405–417
- Shibata K (1957) Spectroscopic studies on chlorophyll formation in intact leaves. *J Biochem* 44:147–173
- Solymosi K, Martinez K, Kristóf Z, Sundqvist C, Böddi B (2004) Plastid differentiation and chlorophyll biosynthesis in different leaf layers of white cabbage (*Brassica oleracea* cv. *capitata*). *Physiol Plant* 121:520–529
- Szenzenstein A, Kósa A, Böddi B (2008) Biological variability in the ratios of protochlorophyllide forms in leaves and epicotyls of dark-grown pea (*Pisum sativum* L.) seedlings (A statistical method to resolve complex spectra). *J Photoch Photobio B* 90:88–94
- Tanaka R, Tanaka A (2007) Tetrapyrrole biosynthesis in higher plants. *Annu Rev Plant Biol* 58:321–346
- Vitányi B, Kósa A, Solymosi K, Böddi B (2013) Etioplasts with protochlorophyll and protochlorophyllide forms in the under-soil epicotyl segments of pea (*Pisum sativum*) seedlings grown under natural light conditions. *Physiol Plant* 148:307–315
- Wilks H, Timko M (1995) A light-dependent complementation system for analysis of NADPH: protochlorophyllide oxidoreductase: identification and mutagenesis of two conserved residues that are essential for enzyme activity. *P Natl Acad Sci USA* 92(3):724–728
- Zhang DW, Yuan S, Xu F, Zhu F, Yuan M, Ye HX, Guo H-Q, Lu X, Yin Y, Lin HH (2014) Light intensity affects chlorophyll synthesis during greening process by metabolite signal from mitochondrial alternative oxidase in *Arabidopsis*. *Plant Cell Environ.* doi:10.1111/pce.12438